



Citation:

---

was 204.2 and 256.2 respectively (Table 1). The result indicated that the activated sample prepared by acid activation possesses good adsorptive capacity. Higher iodine number reflects better development of the microporous structure and higher adsorption abilities [29,30]. It was clear that the iodine number of acid activated adsorbents is high due to the phosphoric acid destroying the aliphatic and aromatic species present in plants therefore swiftly removing the volatile matters during the carbonization process as reported by El-Hendawy [31].

### Scanning electron microscopy (SEM)

The surface morphology of the adsorbent was analyzed by scanning electron microscope (SEM). The results of SEM analysis are shown in the micrographs Figures 1-3. The raw sample in Figure 1 showed rough areas of surface of the carbon and very minute micropores.

It was generally observed that the pore structure development is influenced by many factors, such as inorganic impurities and the initial structure of the carbon precursor [32]. It can clearly be seen in Figure 2 that chemical activation resulted in a porous structure and the opening of pores on the surface of the activated sample.

SEM analysis after adsorption of Cd in Figure 3 however showed a reduced pore sizes as compared to that of the acid activated sample.

### Transmission electron microscopy (TEM)

Transmission electron microscope (TEM) was used to determine the internal morphology of the adsorbent. The results of TEM analysis of the adsorbents, raw sample, activated sample and sample after adsorption are shown in Figures 4-6.

The internal pore size of the raw sample Figure 4 was between 0.94-2.90  $\mu\text{m}$ , those of the activated sample Figure 5 ranged between 5.27-5.92  $\mu\text{m}$ . This improvement in pore size of the activated adsorbent could be due to the carbonization in the presence of acid.

However, after adsorption, the internal pore size of the Cd-embedded adsorbent reduces between 2.43-2.86  $\mu\text{m}$  Figure 6. This observation indicated that the adsorbent is effective on Cd adsorption,

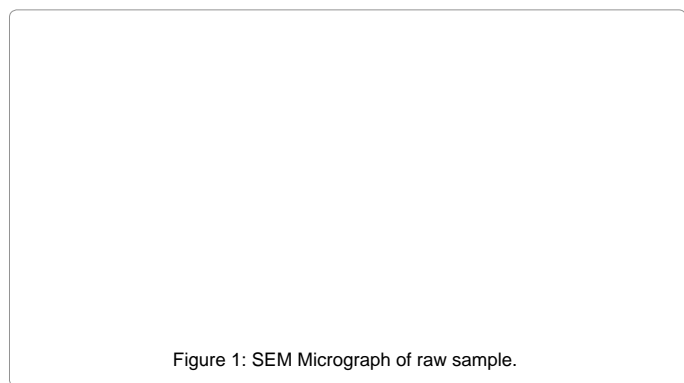



Figure 1: SEM Micrograph of raw sample.

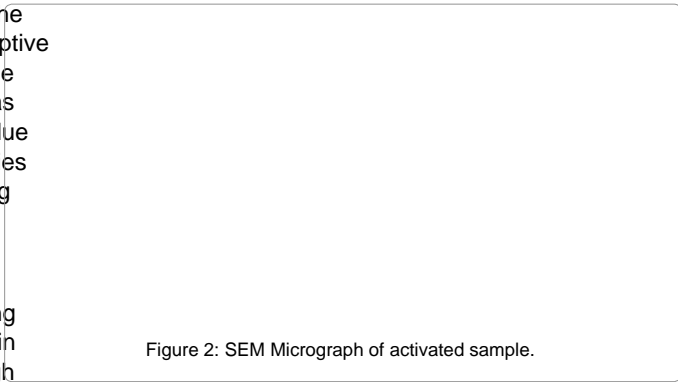


Figure 2: SEM Micrograph of activated sample.

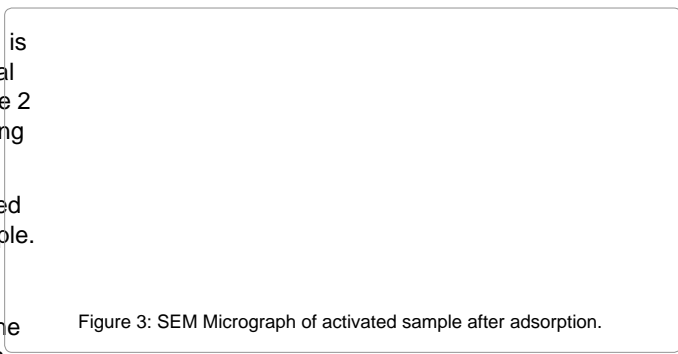


Figure 3: SEM Micrograph of activated sample after adsorption.

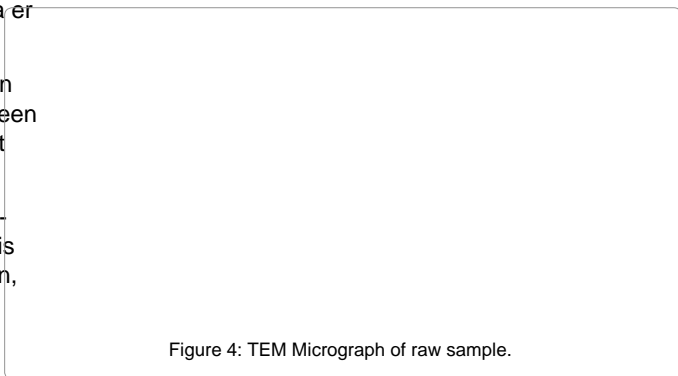


Figure 4: TEM Micrograph of raw sample.

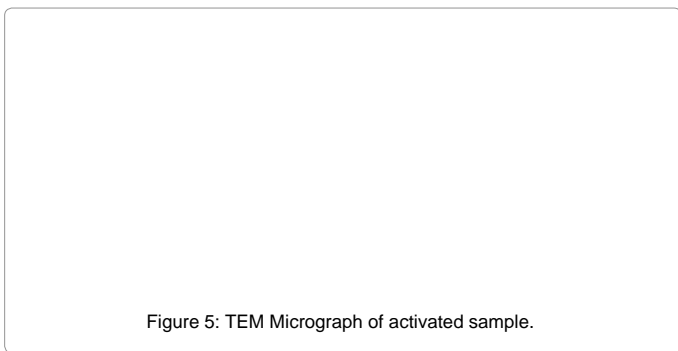


Figure 5: TEM Micrograph of activated sample.

since the internal pore sizes reduced Cd-embedded adsorbent. This implies that Cd ions occupied spaces in adsorbent.

### XRF elemental analysis

The elemental analysis of the adsorbent as revealed by XRF (Table 2) result showed that Ca, Si and Fe are present as major constituents

the modified and metal-loaded adsorbents. These groups might have been destroyed or evaporated during carbonization or converted into another functional group.

The sharp stretch vibrations found within band range 2284-2400  $\text{cm}^{-1}$  appeared to represent functional group of phosphorus belonging to phosphine (P-H). The presence of phosphine group is expected to increase the adsorptive capacity of the adsorbents.

The stretch vibrations of C=O in ketones and aldehydes were found in the range 1700-1735  $\text{cm}^{-1}$  [35]. This peak appeared in raw and Cd-loaded adsorbent but absent in activated adsorbent. This observation may be attributed to the loss of C=O during carbonization process and do not reappear after activation.

Na, Ti and Zn are minor constituents while Mg, Al, P, Mn, Co, Ni, Cu and Cd are in traces.

The bend vibrations of N-H at band range 1450-1550  $\text{cm}^{-1}$

The point of zero charge of activated sample was determined by potentiometry method. The graph of the pH of sample solution and that of the blank solution were plotted as shown in Figure 7. It could be observed that the pH drop for the sample solution and the blank solution intercepted at pH 5.8, this shows that the  $\text{pH}_{\text{pzc}}$  was found to be 5.8 for *vitellaria paradoxa*. Cation adsorption becomes enhanced at higher pH than  $\text{pH}_{\text{pzc}}$ , while adsorption of anions equally enhanced at pH less than  $\text{pH}_{\text{pzc}}$  [33].

#### FTIR Results of the raw sample, activated sample and after adsorption

The comparisons of the Fourier transform infra-red result spectra of raw, modified and after adsorption of the *vitellaria paradoxa* were given in figures. The FTIR spectrum of the raw reveals complex nature of the adsorbent as evidenced by the presence of a large number of peaks. The band between 3000-3500  $\text{cm}^{-1}$  has been assigned to free and intermolecular bonded hydroxyl (O-H) group of alcohol, phenol or carboxyl [34]. These bonds were present in raw, modified and metal-loaded adsorbents; indicating participation of the (O-H) functional group in the metal binding. The peaks at 2918.40  $\text{cm}^{-1}$ , 2046.54  $\text{cm}^{-1}$ , 1633.76  $\text{cm}^{-1}$  and 1427.37  $\text{cm}^{-1}$  have been assigned to C-H, C AC, C AN and C=C respectively in the raw but were completely absent in

trend could be as a result of the increase in the electrostatic interaction between the Cd(II) the adsorbent active sites. Moreover, this can be explained by the fact that more adsorption sites were being covered as the metal ions concentration increases [37]. In the case of low metal ions concentration, the ratio of the initial number of moles of metal ions to the available surface area of the adsorbent is large and subsequently the fractional adsorption becomes independent of initial concentration. However, at higher concentrations, the available sites of adsorption become fewer and hence the percentage removal of metal ions which depends upon the initial concentration decreases [38]. It could however be deduced from the result above the equilibrium concentration is at 200 mg/L.

Effect of pH: The effect of initial solution pH on the adsorption capacity at equilibrium condition was studied. The result for the adsorption of Cd(II) is shown in Figure 8 using 200 mg/L as initial metal concentration. It could be seen that the removal concentration and percentage removal is pH dependent. It was clear that the degree of metal ions adsorption onto the adsorbent increased from 50.48 mg/L to maximum of 57.37 mg/L of Cd(II) when the solution pH was increased from 2-6. However, at the adsorption capacity of the adsorbent

deposited metal ions penetrated to the interior of the adsorbent through intra-particle diffusion which was slower process. This is in accordance with the observation of other similar studies (Figure 10) [40,41].

Effect of temperature: (Figure 8.6)

Citation: Jimoh AA, Adebayo GB, Otun KO, Ajiboye AT, Bale AT, et al. (2015) Sorption Study of Cd(II) from Aqueous Solution Using Activated Carbon Prepared from *Vitellaria paradoxa* Shell. *J Bioremed Biodeg* 6: 288. doi:

---

---

$$\Delta G = \Delta H - T\Delta S \quad (8)$$





Citation: Jimoh AA, Adebayo GB, Otun KO, Ajiboye AT, Bale AT, et al.

---

36. Hu Y, Dong X, Nan J, Jin W, Ren X, et al. (2011) Metal-organic framework membranes fabricated via reactive seeding. *Chem Commun (Camb)* 47: 737-739.
37. /DUDR X V HQLDL \$+ %HQFKHLNK /0 ([SHULPH QWFDORWRSUSTRANPSK028UAPBIDMCO
38. Yu LJ, Shukla SS, Dorris KL, Shukla A, Margrave JL (2003) Adsorption of chromium from aqueous solutions by maple sawdust. *J Hazard Mater* 100: 53-63.
39. Sari A, Tuzen M (2009) Kinetic and equilibrium studies of biosorption of Pb(II) and Cd(II) from aqueous solution by macrofungus (*Amanita rubescens*) biomass. *J Hazard Mater* 164: 1004-1011.
40. Sangi MR, Shahmoradi A, Zolgharnein J, Azimi GH, Ghorbandoost M (2008) Removal and recovery of heavy metals from aqueous solution using *Ulmus FDUSLQLIROLDDQG)UD[LQXVH[FHOVLRU WUHH*
41. Kaiser S, Anwar RS, Muhammad U (2009) Biosorption of lead(II) and chromium(VI) on groundnut hull: Equilibrium, kinetics and thermodynamics study. *Journal of Biotechnology*.
42. Annadural G, Juang RS, Lee DJ (2003) Adsorption of heavy metals from water using banana and orange peels. *Water Sci Technol* 47: 185-190.
43. Garg VK, Gupta R, Kumar R, Gupta RK (2004) Adsorption of chromium from aqueous solution on treated sawdust. *Bioresour Technol* 92: 79-81.
44. Quek SY, Wase DAJ, Forster CF (1998) The Use of Sago Waste for the 6RUSWLRQR I /HDG DQG &RSSHU´ :DWHU 6\$
45. Fuste CM, Pons MP (1993) Uranium uptake by immobilized cells of *QWFDORWRSUSTRANPSK028UAPBIDMCO* *Applied Microbiology Biotechnology* 39: 661-665
46. Langmuir I (1918) The adsorption of gases in plane surfaces of glass, mica and Platinum. *J American Chem Society* 40: 1361-1403.
47. Vijayakumar G, Tamilarasan R, Dharmendirakumar M (2012) Adsorption, kinetic, equilibrium and thermodynamic studies on the removal of basic dye rhodamine-B from aqueous solution by the use of natural adsorbent perlite: *J Mater Environ Sci* 3: 157-170
48. Mohan D, Singh KP (2002) Single and multi-component adsorption of cadmium and zinc using activated carbon derived from bagasse--an agricultural waste. *Water Res* 36: 2304-2318.
49. Hema M, Arivoli S (2007) Comparative study on the adsorption kinetics and thermodynamics of dyes onto acid activated low cost carbon. *Int J Phys Sci* 2: 10-17.
50. Lawal OS, Sanni AR, Ajayi IA, Rabi OO (2010) Equilibrium, thermodynamic and kinetic studies for the biosorption of aqueous lead(II) ions onto the seed husk of *Calophyllum inophyllum*. *J Hazard Mater* 177: 829-835.
51. Chowdhury S, Mishra R, Saha P, Kushwaha P (2011) Adsorption thermodynamics, kinetics and isosteric heat of adsorption of malachite green RQWR FKHPFLFDOO\ PRGL¿HG ULFH KXVN 'HVDOLQD